SOX5 postmitotically regulates migration, postmigratory differentiation, and projections of subplate and deep-layer neocortical neurons

Kenneth Y. Kwan*†, Mandy M. S. Lam*†, Željka Krsnik*, Yuka Imamura Kawasawa*, Veronique Lefebvre‡, and Nenad Šestan*§

*Department of Neurobiology and Kavli Institute for Neuroscience, Yale University School of Medicine, New Haven, CT 06520; and ‡Department of Cell Biology and Orthopaedic Research Center, Lerner Research Institute, Cleveland Clinic, Cleveland, OH 44195

Edited by Yuh Nung Jan, University of California, San Francisco School of Medicine, San Francisco, CA, and approved August 22, 2008 (received for review July 14, 2008)

Neocortical projection neurons exhibit layer-specific molecular profiles and axonal connections. Here we show that the molecular identities of early-born subplate and deep-layer neurons are not acquired solely during generation or shortly thereafter but undergo progressive postmitotic refinement mediated by SOX5. *Fezf2* and *Bcl11b*, transiently expressed in all subtypes of newly postmigratory early-born neurons, are subsequently downregulated in layer 6 and subplate neurons, thereby establishing their layer 5-enriched postnatal patterns. In *Sox5*-null mice, this downregulation is disrupted, and layer 6 and subplate neurons maintain an immature differentiation state, abnormally expressing these genes postnatally. Consistent with this disruption, SOX5 binds and represses a conserved enhancer near *Fezf2*. The *Sox5*-null neocortex exhibits failed preplate partition and laminar inversion of early-born neurons, loss of layer 5 subcerebral axons, and misrouting of subplate and layer 6 corticothalamic axons to the hypothalamus. Thus, SOX5 postmitotically regulates the migration, postmigratory differentiation, and subcortical projections of subplate and deep-layer neurons.

neocortex development | postmitotic mechanisms | pyramidal neurons | *Sox* genes | transcriptional enhancer

The neocortex is composed of six distinct layers, each containing a unique subset of projection (pyramidal) neurons with specific molecular profiles and axonal connectivities (1–3). Subcortical axons arise solely from deep-layer (L5 and L6) neurons, whereas upper-layer (L2–L4) neurons project intracortically. The first projection neurons, born from progenitors in the ventricular zone (VZ) (4, 5), migrate radially and settle within the preplate (PP), where they form the nascent cortical plate (CP) (6). Incoming CP neurons, which split the PP into the marginal zone (MZ) and subplate (SP), are generated sequentially so that early-born neurons occupy the deep layers and later-born neurons migrate past older neurons to settle in more superficial layers. The molecular mechanisms that regulate the laminar position and identity of projection neurons are being unraveled (3, 7). Previous studies suggested that neurons are specified at the time of their birth (2, 8). However, the extent to which postmitotic events contribute to their laminar and molecular identity remains an open question.

Fezf2 (*Fezl* or *Zfp312*) and *Bcl11b* (*Ctip2*) encode transcription factors enriched in and necessary for the development of L5 neurons (9–12). Here we show that the L5-enriched postnatal expression patterns of *Fezf2* and *Bcl11b* are not acquired solely during neuronal generation but rather are the result of progressive refinement during postmigratory differentiation mediated by SOX5 (L-SOX5), a transcription factor that has been shown to regulate chondrogenesis, oligodendrogenesis, and the sequential generation of cortical neurons (13–16). In this study, we show that *Sox5* postmitotically controls the laminar positioning, molecular differentiation, and layer-specific pattern of subcortical axonal projections of SP and deep-layer neurons.

Results

SOX5 Expression in SP and L6 Projection Neurons Coincides with *Fezf2* Downregulation. From a previous microarray screen (12), we selected *Sox5* for further studies based on its distinct early-postnatal expression pattern in the deep neocortical layers: high in SP and L6, and lower in L5. This pattern was opposite to *Fezf2* expression, which was highest in L5 and weaker in L6 and SP (12). To examine the expression of SOX5 in relation to *Fezf2* during cortical development, we used the *Fezf2-Gfp* BAC transgenic mouse (*Fezf2-Gfp*) (17), in which GFP is expressed in a *Fezf2* pattern (Fig. 1). At embryonic day 12.5 (E12.5), SOX5 was present in PP neurons but was absent from VZ progenitors and migratory CP neurons, both of which highly expressed *Fezf2-Gfp*. Although at E14.5 SOX5 was expressed only weakly in newly postmigratory L6 and SP neurons, SOX5 was upregulated markedly in these neurons starting at E16.5. Coincidently, *Fezf2*, which was highly expressed by SP, L6, and L5 neurons at E14.5, was greatly downregulated in SP and L6 neurons by E16.5, thereby creating the L5-enriched expression pattern observed at postnatal day 0 (P0). These concurrent reciprocal changes in SOX5 and *Fezf2* expression in SP and L6 neurons suggest that these genes are functionally related. This suggestion is also supported by the evolutionary conservation of these complementary patterns in the mid-fetal human neocortex [supporting information (SI) Fig. S1]. Retrograde axonal tracing further revealed that at P7, SOX5 was expressed by a great majority of corticothalamic and corticospinal neurons and by a small proportion of callosal projection neurons in the deep layers (Fig. S2). Together, these results show that SOX5 is expressed in different subclasses of projection neurons, and its expression in SP and L6 neurons is associated with the postmigratory downregulation of *Fezf2*.

Neocortical *Fezf2* Expression Is Altered in *Sox5* KO Mice. The complementary spatiotemporal expression patterns of SOX5 and *Fezf2* suggest that SOX5 might regulate *Fezf2* expression. Therefore, we analyzed *Fezf2* expression in *Sox5*-null mice (KO; −/−), which exhibit a cleft palate and die hours after birth (13). Strikingly, in P0 KO neocortex, the pattern of *Fezf2* mRNA and *Fezf2-Gfp* expression was shifted compared with heterozygotes (Het; +/−), with the highest levels in the deepest part of the KO neocortex (Fig. 2*A*).

Author contributions: K.Y.K., M.M.S.L., V.L., and N.S. designed research; K.Y.K., M.M.S.L., Z.K., and Y.I.K. performed research; V.L. contributed new reagents/analytic tools; K.Y.K., M.M.S.L., and N.S. analyzed data; and K.Y.K., M.M.S.L., and N.S. wrote the paper.

The authors declare no conflict of interest.

This article is a PNAS Direct Submission.

†K.Y.K. and M.M.S.L. contributed equally to this work.

§To whom correspondence should be addressed at: Department of Neurobiology, Yale University School of Medicine, 333 Cedar Street, SHM C-323C, New Haven, CT 06510. E-mail: nenad.sestan@yale.edu.

This article contains supporting information online at www.pnas.org/cgi/content/full/0806791105/DCSupplemental.

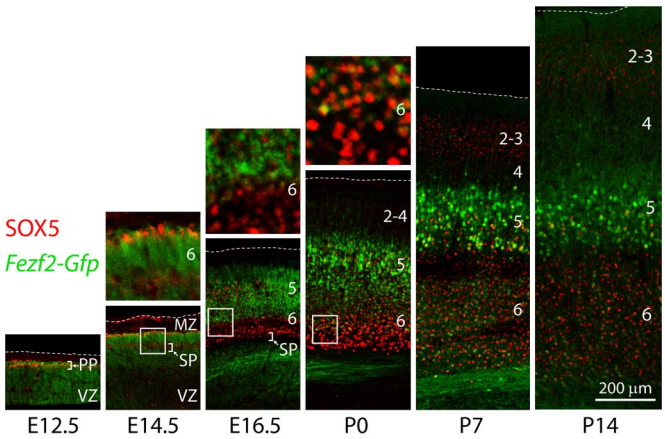

Fig. 1. SOX5 up-regulation in postmigratory SP and L6 neurons coincides with *Fezf2* downregulation. Neocortex of *Fezf2-Gfp* (*green*) transgenic mice immunostained for SOX5 (*red*). Dashed lines indicate pial surface. At E12.5, SOX5 is expressed in PP neurons but not in *Fezf2-Gfp*-positive VZ progenitors. At E14.5, SOX5 is weakly expressed in *Fezf2-Gfp*-positive postmigratory CP neurons. Starting at E16.5, concomitant with *Fezf2-Gfp* downregulation, SOX5 expression is upregulated in SP and L6 neurons. At early postnatal ages, SOX5 is expressed in most SP and L6 neurons and in some L5 and L2-3 neurons, whereas *Fezf2* is expressed highly in L5 neurons and weakly in L6 and SP neurons.

More importantly, *Fezf2* mRNA expression, analyzed by quantitative RT-PCR, was significantly increased about twofold in the KO neocortex (Fig. 2*B*). These data indicate that *Fezf2* expression is upregulated in the absence of *Sox5*, and its normal L5-enriched pattern is shifted toward deeper parts of the neocortex, consistent with a role of SOX5 in repressing *Fezf2* in SP and L6 neurons.

SOX5 Binds and Represses an Evolutionarily Conserved Enhancer Near the *Fezf2* Gene. To explore a mechanism by which SOX5 represses *Fezf2* expression, we examined putative regulatory sequences near the *Fezf2* genomic locus. An evolutionarily conserved region (434 enhancer) downstream of the human *FEZF2* transcription start site exhibits enhancer activity resembling the pattern of *Fezf2* in E11.5 transgenic mice (VISTA Enhancer Browser) (Fig. S3*A–C*) (18). Furthermore, the orthologous mouse sequence exhibited activity in deep-layer neurons similar to endogenous *Fezf2* expression (Fig. S3*D*). These results, although not definitive, suggest that this enhancer regulates *Fezf2* transcription. Analysis using MatInspector revealed that this putative *Fezf2* regulatory element contains two pairs of highly conserved consensus binding sites for SOX5 (Fig. 2*C*). To determine SOX5 binding of these sites, we performed chromatin immunoprecipitation (ChIP) with cortices dissected from P0 mice, using KO mice to control for possible nonspecific antibody binding ($n = 2$ per genotype). Both of the anti-SOX5 antibodies used specifically precipitated this DNA in Het but not KO mice, confirming *in vivo* binding of SOX5 (Fig. 2*D*). To test whether SOX5 binding has functional consequences, we cloned the 82-bp sequence containing both pairs of SOX5 binding sites, as well as mutated versions thereof, downstream of the luciferase reporter gene for luciferase assays in N2a cells (Fig. 2*E* and *F*). SOX5 significantly repressed the activity of the wild-type enhancer by 51.5% ± 1.7%. Mutating the binding sites rescued the repression to varying degrees, whereas mutations in all four sites rescued the repression almost completely. Collectively, these results indicate that SOX5 binds to and represses the activity of a conserved enhancer element proximal to the *Fezf2* locus.

Alterations in Expression Pattern of Subplate and Deep-Layer Markers in *Sox5* KO Neocortex. Next, we analyzed the cytoarchitecture and marker expression of the P0 KO brain. Nissl staining revealed no gross structural abnormalities (Fig. S4). However, a well-delineated SP was absent in the KO neocortex. The expression of RELN, a marker of layer 1 (19), was not affected (Fig. S5*A*). Expression of *Ctgf*, a marker of SP (20), was reduced dramatically in the KO neocortex. *Tle4*, a marker of L6 and SP (21), was unperturbed in deep CP but was largely lost below, where the SP normally is

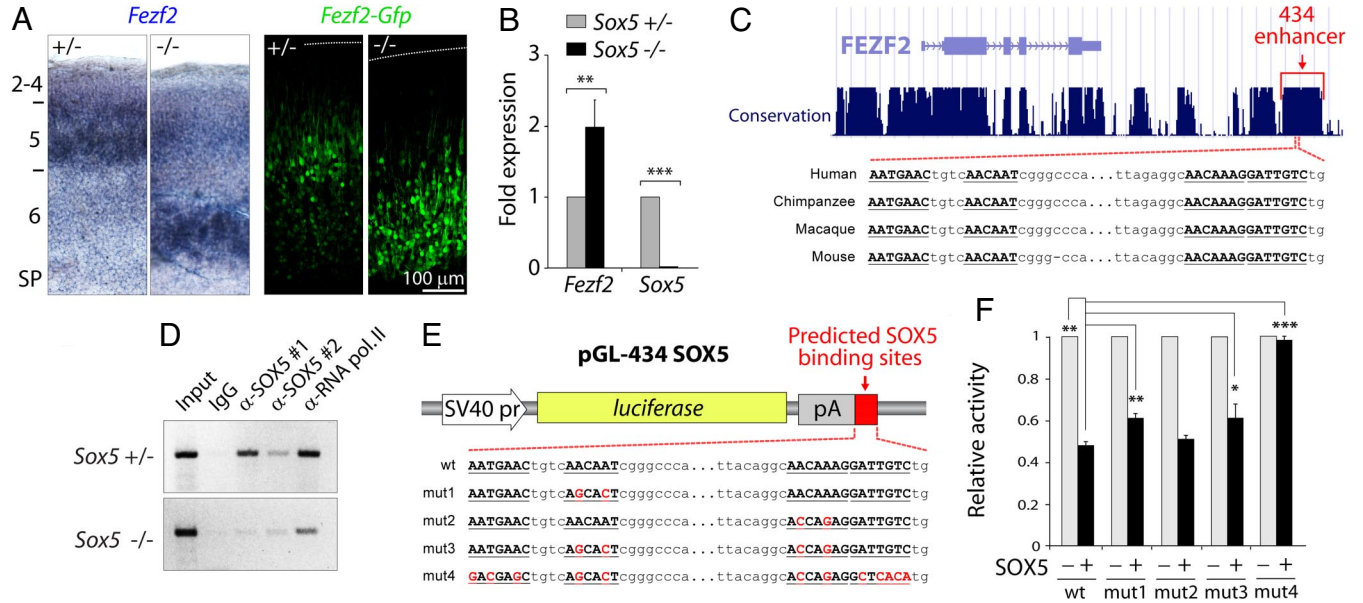

Fig. 2. SOX5 regulates *Fezf2* expression and binds and represses the activity of a conserved enhancer near *Fezf2*. (*A*) In P0 *Sox5*−/− neocortex, *Fezf2* mRNA and *Fezf2-Gfp* expression were shifted toward deeper laminar positions. $n \geq 2$ per genotype. (*B*) Quantitative RT-PCR of neocortical mRNA normalized to *Gapdh*. *Fezf2* mRNA levels increased 2.0 ± 0.39-fold in *Sox5*−/− neocortex. $n = 2$ per genotype. (*C*) Evolutionary conservation of the human 434 enhancer region and predicted SOX5 binding sites (*underlined*). (*D*) ChIP assays in P0 cortices. DNA fragments immunoprecipitated with IgG, anti-SOX5, or anti-RNA polymerase II antibodies were analyzed by PCR with primers specific for the predicted SOX5 sites. (*E*) Luciferase constructs used in (*F*). Wild-type (wt) or mutated (mut) (*red*) SOX5 binding sites (*underlined*) were inserted downstream of luciferase. (*F*) Luciferase assays in N2a cells transfected with pCAG-*Sox5* (*black bars*) or empty pCAGEN (*gray bars*). *Sox5* repressed luciferase activity of wt and mut1–4 constructs by 51.5% ± 1.7%, 39.7% ± 2.5%, 49.6% ± 1.8%, 39.5% ± 6.7%, and 0.06% ± 0.01%, respectively. $n = 6$ per condition. Error bars represent 95% confidence levels. Student's *t* test, $^*P < 0.05$; $^{**}P < 0.01$; $^{***}P < 0.001$.

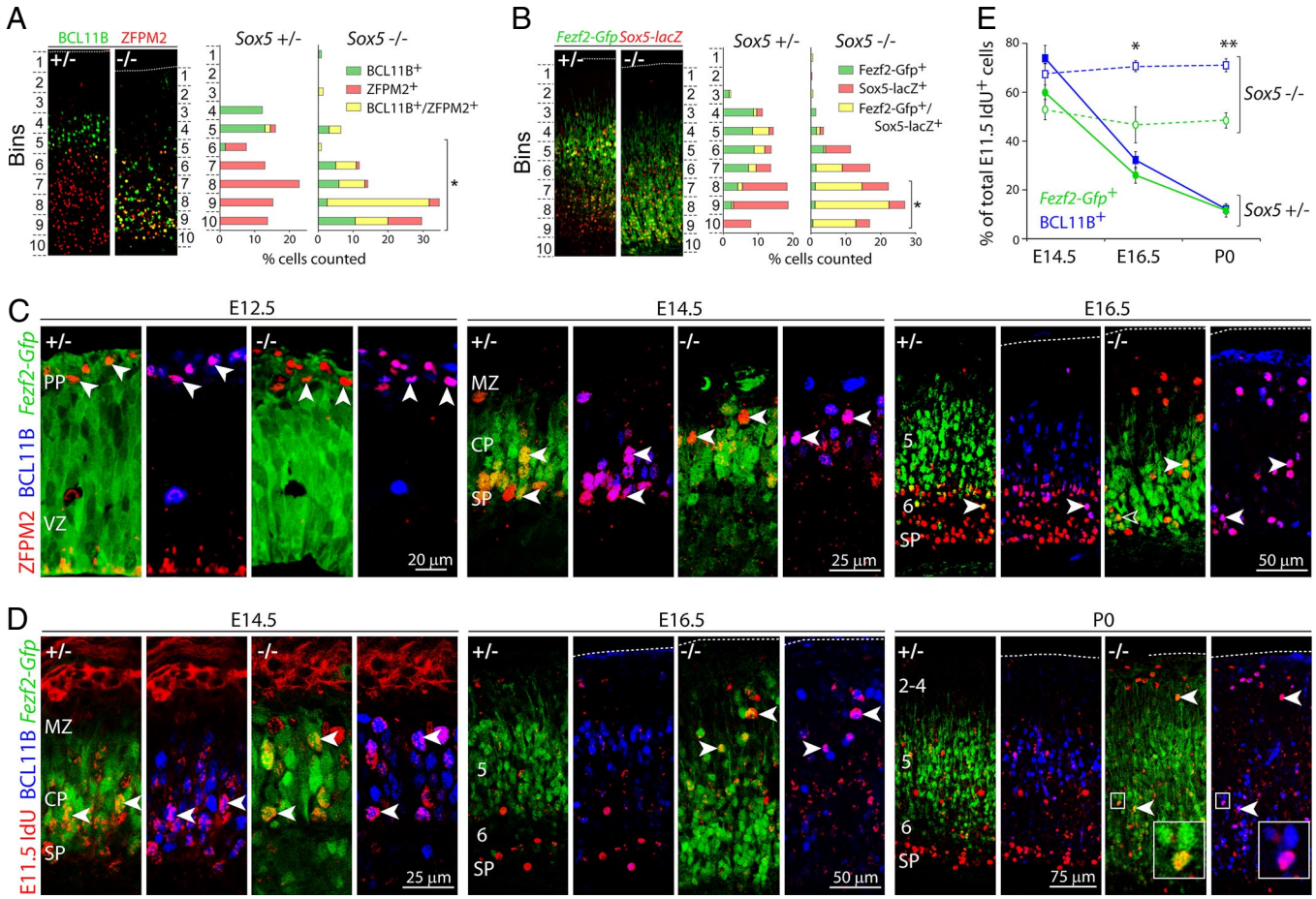

Fig. 3. Postmigratory downregulation of *Fezf2* and BCL11B in SP and L6 neurons requires SOX5. (*A*) At P0, BCL11B (*green*) and ZFPM2 (*red*) were coexpressed (*yellow*) in the deep layers in only a small proportion of neurons in *Sox5*+/− neocortex but in a large proportion of neurons in *Sox5*−/− neocortex. $n = 2$ per genotype. (*B*) At P0, lacZ (*red*) expressed from the *Sox5* locus and *Fezf2-Gfp* (*green*) were coexpressed (*yellow*) rarely in *Sox5*+/− but extensively in *Sox5*−/− neocortex. $n = 3$ per genotype. (*C*) At E12.5 and E14.5, ZFPM2-positive neurons (*red*) co-expressed high levels of *Fezf2-Gfp* (*green*) and BCL11B (*blue*) in both *Sox5*+/− and *Sox5*−/− neocortex. At E16.5, ZFPM2-positive neurons downregulated *Fezf2-Gfp* and BCL11B in *Sox5*+/− but not in *Sox5*−/− neocortex. (*D*) Neurons born at E11.5 were labeled by injection of IdU (*red*). At E14.5, IdU-labeled neurons co-expressed high levels of *Fezf2-Gfp* and BCL11B in both *Sox5*+/− and *Sox5*−/− neocortex. At E16.5, IdU-labeled neurons downregulated *Fezf2-Gfp* and BCL11B in *Sox5*+/− but not *Sox5*−/− neocortex. At P0, high levels of *Fezf2-Gfp* and BCL11B remained in IdU-labeled neurons in *Sox5*−/− neocortex. (*E*) Quantitative analysis of cells labeled by E11.5 IdU injection expressing BCL11B (*blue lines*) and *Fezf2-Gfp* (*green lines*) in *Sox5*+/− (*solid lines*) and *Sox*−/− (*dashed lines*) neocortex. $n = 2$ per genotype. Error bars represent S.E.M. Student's *t* test, $*P < 0.05$, $**P < 0.01$.

NEUROSCIENCE

situated (Fig. S5*B*). ZFPM2 (FOG2) (12) and TBR1 (22), both normally expressed in L6 and SP neurons, exhibited slightly reduced expression in the KO neocortex. A number of ZFPM2- and TBR1-expressing neurons were positioned ectopically in the upper layers (Fig. S5*B*). Analysis of L5 markers BCL11B (10) and ETV1 (ER81) (23) showed striking shifts toward deeper positions in the KO neocortex, similar to *Fezf2* (Fig. S5*C*). However, in lateral KO neocortex, BCL11B was dramatically downregulated, and the ETV1 shift was less prominent (data not shown), indicating possible alterations in areal patterning. *Rorb*, a marker of L4 (24), and CUTL1 (CUX1) (25), a marker of the upper layers, were largely unaffected (Fig. S5*D*). These data show that loss of SOX5 specifically affects deep-layer gene expression, decreasing the expression of SP and L6 markers and shifting the expression of BCL11B, ETV1, and *Fezf2* from L5 to deeper positions in the neocortex.

Deep-Layer Neurons Exhibit Mixed Molecular Properties in *Sox5* KO Neocortex. To examine the molecular properties of the KO neocortex further, we analyzed whether markers typically selective for L5 or L6 became abnormally coexpressed. At P0, BCL11B and ZFPM2 normally are highly expressed in L5 and L6, respectively, with little overlap. To quantify their co-expression, the distribution of cells singly expressing BCL11B or ZFPM2 or co-expressing both was analyzed (Fig. 3*A*). In the KO neocortex, the number of cells co-expressing BCL11B and ZFPM2 increased significantly compared with the Het neocortex. Because Het and KO mice express lacZ from the *Sox5* locus in a *Sox5* pattern, lacZ staining was used to mark neurons that normally would express *Sox5*. In the Het neocortex, *Fezf-Gfp* was expressed only occasionally in lacZ-expressing neurons. In the KO neocortex, lacZ-expressing neurons co-expressed *Fezf2-Gfp* extensively (Fig. 3*B*), indicating an upregulation of *Fezf2* in these cells in the absence of *Sox5*. In a very small number of KO mice that survived past birth (4 of > 200 KO mice), possibly because of variability in cleft palate severity, BCL11B, ZFPM2, and *Fezf2-Gfp* co-expression persisted at P7 (Fig. S6*A*). Collectively, these data indicate that some neurons in the KO neocortex exhibit abnormal mixed molecular properties of both L5 and L6. However, numerous neurons maintained normal single expression of BCL11B or ZFPM2, indicating that not all deep-layer neurons became molecularly mixed in the KO neocortex.

SP and L6 Neurons Fail to Down-Regulate *Fezf2* and BCL11B in *Sox5* KO Neocortex During Late Embryonic Development. The mixed molecular identities of neurons in the postnatal KO neocortex could be

caused by abnormal induction of BCL11B and *Fezf2* or by their failed downregulation after transient expression. The latter possibility is supported by the downregulation of initially high *Fezf2* expression in normal SP and L6 neurons between E14.5 and E16.5 (Fig. 1). Therefore, we examined the co-expression of *Fezf2-Gfp*, BCL11B, and ZFPM2 during embryonic development. Remarkably, in the E12.5 and E14.5 Het neocortex, before the onset of high SOX5 expression, the majority of ZFPM2-expressing PP, SP, and L6 neurons co-expressed high levels of *Fezf2-Gfp* and BCL11B (Fig. 3*C*). Coinciding with increased SOX5 expression in SP and L6 at E16.5, BCL11B and *Fezf2-Gfp* expression showed reduced overlap with ZFPM2, indicating that the postnatal expression patterns of these markers were acquired progressively through the downregulation of *Fezf-Gfp* and BCL11B by ZFPM2-expressing SP and L6 neurons. We further confirmed that this downregulation occurred intrinsically by birth-dating SP and L6 neurons born at E11.5 with 5-iodo-2-deoxyuridine (IdU). In Het neocortex, a large proportion of neurons born at E11.5 expressed high levels of *Fezf2-Gfp* or BCL11B at E14.5 (59.9% ± 6.5% and 73.9% ± 5.3%, respectively) (Fig. 3*D* and *E*), whereas a smaller proportion did so at E16.5 (26.0% ± 3.3% and 32.2% ± 3.4%). By P0, only a small proportion of these neurons expressed either gene at detectable levels (11.6% ± 2.7% and 12.2% ± 2.1%).

In the E12.5 and E14.5 KO neocortex, *Fezf2-Gfp*, BCL11B and ZFPM2 were co-expressed in CP neurons, as found in Het neocortex (Fig. 3*C*). However, this co-expression was aberrantly maintained at high levels in the E16.5 and P0 KO neocortex (Fig. 3*C* and data not shown). Similarly, the proportion of E11.5 IdU-labeled neurons highly expressing *Fezf2-Gfp* or BCL11B in the E14.5 KO neocortex (52.9 ± 4.2% and 67.4 ± 4.4%, respectively) (Fig. 3*D* and *E*) was comparable to that in the Het neocortex. However, a high proportion of these neurons maintained strong expression of *Fezf2-Gfp* or BCL11B at E16.5 (46.6% ± 7.4% and 70.7% ± 2.2%, respectively) and P0 (48.4% ± 3.1% and 71.0% ± 2.6%, respectively), indicating that these genes were not downregulated appropriately.

Collectively, these data indicate that newly postmigratory SP and L6 neurons transiently expressed and, during differentiation, progressively downregulated molecular markers postnatally enriched in L5 neurons. The timing of this postmitotic refinement coincides with the upregulation of SOX5 expression in these neurons, and in the KO neocortex postnatal *Fezf2-Gfp* and BCL11B expression is maintained abnormally in SP and L6 neurons because of the failure of this downregulation.

Laminar Positioning Defects of Subplate and Deep-Layer Neurons in *Sox5* KO Neocortex. The ectopic ZFPM2- and TBR1-expressing neurons in the upper layers of the KO neocortex suggest alterations in neuronal migration. Therefore, we used 5-chloro-2-deoxyuridine (CldU) and IdU to birth-date SP and deep-layer neurons at E11.5, E12.5, and E13.5 ($n = 3$ per genotype) and upper-layer neurons at E15.5 and E16.5 ($n = 2$) and then analyzed their radial distribution at P0 (Fig. S7). In the KO neocortex, neurons labeled at E11.5 and E12.5 shifted dramatically away from the SP toward more superficial layers. Many E11.5-labeled neurons were positioned immediately below layer 1, suggesting that some SP neurons were not separated from the MZ during PP splitting, as shown by Lai *et al.* (14). The distribution of upper-layer neurons labeled at E15.5 and E16.5 were normal in the KO cortex, indicating that the migration defects in the KO cortex specifically affected early-born SP and deep-layer neurons.

Aberrant Preplate Splitting Caused by Premature Migration Arrest in *Sox5* KO Neocortex. To analyze further the partitioning of the PP, we examined expression of PP, SP, and L6 markers at E14.5 (Fig. 4*A*). In the Het neocortex, MAP2 expression formed distinct bands in the MZ and SP. In the KO neocortex, SP expression of MAP2 is

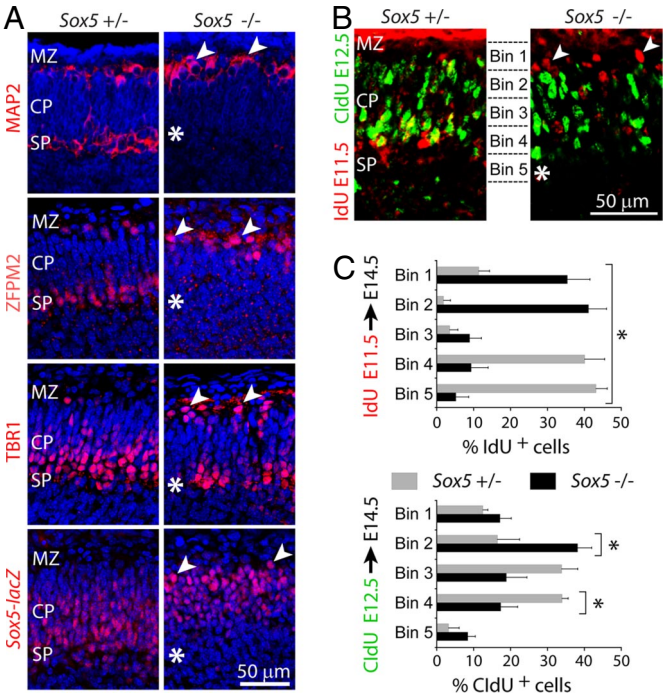

Fig. 4. Failed preplate splitting caused by premature migration arrest of early-born neurons in *Sox5* KO neocortex. (*A*) E14.5 neocortex immunostained with indicated antibody (*red*) and counterstained (*blue*). In *Sox5*−/− mice, neurons expressing SP markers were ectopically present in the upper portion of CP (*arrowheads*). The expected location of SP in the KO neocortex is indicated (*asterisks*). (*B*) E14.5 neocortex of embryos injected with IdU (*red*) at E11.5 and CldU (*green*) at E12.5. In *Sox5*+/− neocortex, IdU-labeled cells were positioned below CldU-labeled cells in the SP. In *Sox5*−/− neocortex, IdU-labeled cells (*arrowheads*) were ectopically positioned in the upper CP and above CldU-labeled cells. (*C*) Radial distribution of IdU- and CldU-labeled cells. $n = 3$ per genotype. Error bars represent S.E.M. Student's *t* test, $^*P < 0.05$.

lost, and the domain of MAP2 expression in the MZ is expanded. The expression of ZFPM2, TBR1, and lacZ shifted to the upper edge of the CP, immediately below the MZ. To investigate further the relative positions of early-born SP and L6 neurons, we injected IdU at E11.5 and CldU at E12.5 and examined labeled cells at E14.5 (Fig. 4*B* and *C*). In the Het neocortex, cells labeled at E11.5 occupied the SP, with those labeled at E12.5 immediately above in the SP and deep CP. In the KO neocortex, cells labeled at E11.5 occupied the upper edge of the CP (Fig. 4*B*), immediately below the MZ, whereas those labeled at E12.5 were positioned just below. Therefore, in the KO neocortex, neurons born at E12.5 failed to migrate past those born 1 day earlier, prematurely arresting immediately below and resulting in failed PP splitting and an inversion of the early-born neurons.

Loss of Subcerebral and Misrouting of Corticothalamic Projections in *Sox5* KO Mice. The KO defects in SP, which is critical for proper targeting of subcortical axons (26, 27), prompted us to investigate whether projections were altered. To analyze layer-specific projections, we anterogradely traced subcortical axons using GFP expressed from two layer-specific transgenes; *Fezf2-Gfp*, highly expressed in L5 neurons, and *Golli-Gfp*, exclusively expressed in SP and L6 neurons (28). In the P0 Het brain, both *Fezf2-Gfp*- and *Golli-Gfp*-positive corticothalamic axons were abundantly present and invaded the dorsal thalamus via separate paths (Fig. 5*A* and *C*). In the KO brain, *Fezf-Gfp*-positive axons reaching the dorsal thalamus were greatly reduced, and their paths in the internal capsule lacked stereotypical organization (Fig. 5*A*). Strikingly, *Golli-Gfp*-positive axons failed to enter the

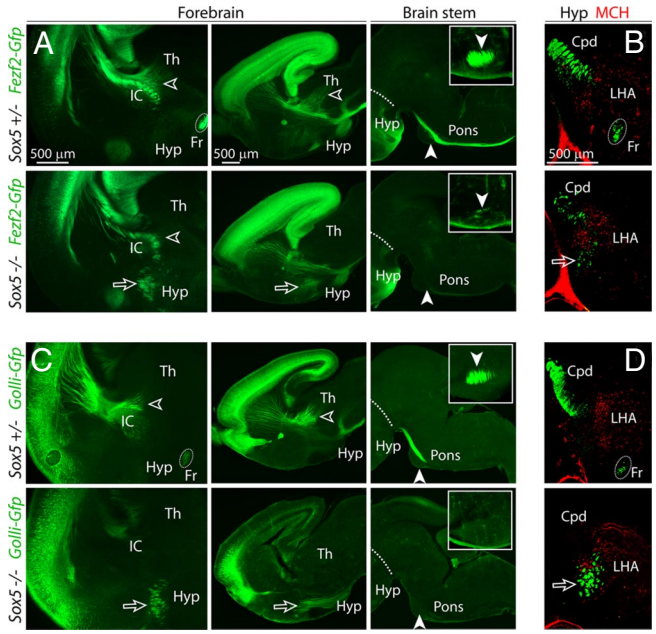

Fig. 5. Loss of L5 subcerebral projections and misrouting of SP and L6 projections into the hypothalamus of *Sox5* KO mice. *Fezf2-Gfp*-positive axons (*green*, *A* and *B*) originate mainly from L5, and *Golli-Gfp*-positive axons (*green*, *C* and *D*) arise from L6 and SP. At P0, *Sox5*−/− mice exhibited loss of internal capsule (IC) organization, a dramatic decrease of *Fezf2-Gfp*-positive axons (*A*), and complete loss of *Golli-Gfp*-positive axons (*C*) in dorsal thalamus (Th) (*open arrowheads*), fornix (Fr), and pons (*solid arrowheads*). An aberrant tract containing both *Fezf2-Gfp*-positive and *Golli-Gfp*-positive axons was misrouted to the hypothalamus (Hyp) (*arrows*). Dashed lines indicate the forebrain-midbrain border. $n > 5$ per genotype. (*B* and *D*) Coronal sections through the caudal cerebrum immunostained for melanin-concentrating hormone (MCH) (*red*), a marker of the LHA. In *Sox5*−/− mice, the *Fezf2-Gfp*-positive and *Golli-Gfp*-positive axons deviated from the cerebral peduncle (Cpd) and aberrantly entered the LHA (*arrows*).

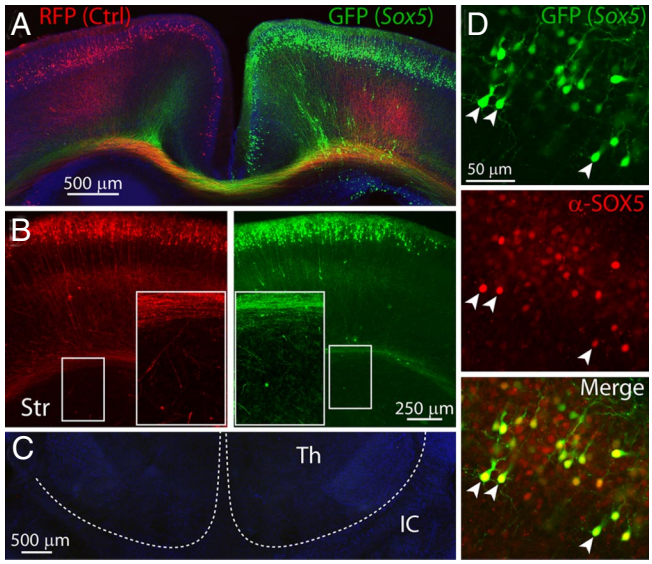

Fig. 6. *Sox5* overexpression is insufficient to respecify upper-layer callosal projections or induce ectopic subcortical projections. Both control RFP-positive axons (*red*) and SOX5-overexpressing GFP-positive axons (*green*) abundantly crossed the corpus callosum (*A*) and, to a small extent, entered the upper striatum (Str) (*B*). (*C*) Neither RFP-positive nor GFP-positive axons projected to the thalamus (Th) or internal capsule (IC). (*D*) Immunostaining for SOX5 (*red*) confirmed high expression of SOX5 in virtually all GFP-positive neurons (*arrowheads*) and weak endogenous SOX5 expression in some GFP-negative upper-layer neurons.

internal capsule, and none reached the dorsal thalamus (Fig. 5*C*). Sections through the pons revealed tightly bundled *Fezf-Gfp*-positive subcerebral axons in the Het mice (Fig. 5*A*). In the KO mice, only a few small bundles of *Fezf-Gfp*-positive subcerebral axons reached the pons. Although numerous *Golli-Gfp*-positive axons innervated the pons in the Het mice, none reached any subcerebral levels in the KO mice (Fig. 5*C*).

Analysis of KO brain also revealed numerous misrouted *Fezf-Gfp*- and *Golli-Gfp*-positive axons, most prominently an aberrant tract misdirected into the hypothalamus (Fig. 5*A* and *C*), indicating defects in axonal pathfinding. At caudal levels of the Het cerebrum, *Fezf-Gfp*- and *Golli-Gfp*-positive axons were present in the cerebral peduncles but not in the lateral hypothalamic area (LHA) marked by immunostaining for melanin-concentrating hormone (Fig. 5*B* and *D*) (29). In the KO caudal cerebrum, however, *Fezf-Gfp*- and *Golli-Gfp*-positive axons were significantly reduced in the cerebral peduncles and aberrantly invaded the LHA. Serial sections through the rostral midbrain revealed that these aberrant axons were not present at any subcerebral levels (data not shown), indicating that they terminated within the hypothalamus. These axon defects, which persisted in P7 KO mice (Fig. S6*B*), were confirmed pancortically using the *Emx1-Cre*;*CAG-Cat-Gfp* transgenic mice (30) that expressed GFP in axons arising from all cortical projection neurons (Fig. S8*A*–*C*) and by immunostaining for L1-CAM (Fig. S6*B*). Furthermore, diotadecyl-tetramethylindocarbocyanine (DiI) retrograde tracing from the dorsal thalamus confirmed a significant decrease in corticothalamic axons and revealed a shift in their laminar origin in the KO mice (Fig. S8*D*–*F*), consistent with migration defects. Taken together, these data indicate that multiple subcortical projections were reduced dramatically and were misrouted to the hypothalamus in the KO mice. This disruption was layer specific, affecting axons arising from SP and L6 neurons more severely than those from L5. Importantly, despite aberrant maintenance of *Fezf2* and BCL11B expression, L6 and SP neurons did not acquire the subcerebral connectivity of L5 neurons in the KO mice.

***Sox5* Is Insufficient to Induce Ectopic Subcortical Axonal Projections or Respecify Normal Callosal Projections.** To determine whether SOX5 is intrinsically sufficient to induce subcortical axonal projections, we carried out *in utero* electroporation (31) at E15.5 to overexpress SOX5 specifically in upper-layer neurons (Fig. 6). To control for timing of injection, a *Sox5* overexpression construct with the GFP reporter was injected into one cortical hemisphere, and a control RFP construct was injected into the contralateral hemisphere ($n = 4$). At P7, SOX5 overexpression was confirmed in electroporated GFP-expressing neurons by immunofluorescent staining (Fig. 6*D*). Some surrounding neurons endogenously expressed low levels of SOX5, confirming that SOX5 is weakly expressed by normal upper-layer neurons at this age (Fig. 1). Both control RFP-positive and SOX5-overexpressing GFP-positive neurons exhibited typical pyramidal morphology and normal radial distribution (Fig. 6*A*). Analysis of projections revealed that SOX5-expressing GFP-positive axons were indistinguishable from RFP control, abundantly entering the corpus callosum and extending short branches to the upper striatum (Fig. 6*A* and *B*), consistent with previous data that some upper-layer neurons normally extend short axon branches to the dorsal striatum (12, 32). Neither RFP- nor GFP-expressing axons reached the internal capsule or thalamus or any subcerebral levels (Fig. 6*C*). Consistently, overexpression of SOX5 by electroporation at E12.5 and E14.5 (data not shown) also failed to suppress callosal axons or induce additional subcortical projections. Together, these results show that SOX5 overexpression is not sufficient to respecify callosal projections or to induce ectopic subcortical axonal projections.

Discussion

In this study, we show that SOX5 postmitotically controls the molecular identity, laminar positioning, and axonal connectivity of

NEUROSCIENCE

early-born neocortical projection neurons. Our data revealed that laminar-specific neuronal identities are not acquired solely during neuron birth but rather are refined by SOX5 during postmigratory differentiation. Specifically, we show that *Fezf2* and *Bcl11b* transiently exhibit broader expression in newly postmigratory SP, L6, and L5 neurons and subsequently undergo SOX5-dependent progressive refinement to establish their postnatal L5-enriched patterns. Consistent with this function, SOX5 binds and represses a conserved enhancer near the *Fezf2* locus. In the absence of *Sox5*, this downregulation fails, and strong expression of *Fezf2* and *Bcl11b* thus remains in postnatal SP and L6 neurons (Fig. S9*A*). This downregulation of transient *Fezf2* or *Bcl11b* expression is distinct from mechanisms that suppress them in upper-layer neurons, which do not express these genes at any time during development (33, 34), but is consistent with a wider role of transcriptional repression in controlling neuronal identities (35).

In addition to postmigratory differentiation, we also showed that *Sox5* is required for newborn deep-layer but not upper-layer neurons to migrate past earlier-born neurons. In the *Sox5* KO neocortex, PP segregation failed, and the deep layers were specifically inverted. The onset of SOX5 expression during the final stage of migration in some CP neurons is consistent with a cell-autonomous role in this process. However, it also is possible that abnormalities in SP development can affect migration in a manner that is not cell autonomous. Interestingly, neurons deficient in *Fezf2* or *Bcl11b* (9–12) or overexpressing *Fezf2* (12) do not exhibit migration defects, suggesting additional targets downstream of SOX5.

Furthermore, layer-specific anterograde tracing revealed that, in the *Sox5* KO brain, corticothalamic and subcerebral axons originating from L5 neurons are severely reduced, whereas those arising from SP and L6 neurons are lost almost completely and are misrouted to the hypothalamus (Fig. S9*B*). Our model of *Sox5* function contrasts with that of Lai *et al.* (14), who recently proposed that the sequential generation of corticofugal neurons is accelerated in the *Sox5* KO brain, so that L5 subcerebral neurons are generated in place of SP and L6 neurons because of the premature induction of BCL11B expression, leading to exuberant subcerebral projections. Our data show that SOX5 is required for the postmitotic downregulation of transient *Fezf2* and BCL11B expression in SP and L6 neurons, a mechanism distinct from premature induction. Moreover, our pan-cortical anterograde tracing further revealed a marked overall reduction in subcerebral projections in the *Sox5* KO brain.

In conclusion, our data indicate that classic aspects of neuronal identity such as laminar position and gene expression are not solely or terminally specified during the birth of neurons from progenitors or shortly thereafter. Rather, postmitotic events also are required to refine their distinct identities. Thus, our study indicates that both pre- and postmitotic molecular mechanisms contribute to the acquisition of laminar position, neuronal identity, and connectivity in the cerebral cortex.

Materials and Methods

Animals. All experiments were carried out in accordance with a protocol approved by the Yale Committee on Animal Research.

Luciferase Assays. N2a cells were transfected with pCAG-*Sox5* or empty pCAGEN, firefly luciferase (pGL3) containing wild-type or mutated SOX5 binding sites and Renilla luciferase (pRL-SV40) and were assayed 48 h later.

Chromatin Immunoprecipitation. P0 cortices of KO and Het mice were minced, cross-linked with 1 mM disuccinimidyl glutarate and 1% formaldehyde, and processed using EZ-ChIP (Millipore). Capture of the enhancer region was tested by PCR using primers ChIP-F, TGGACTTTTCTTTTCTGCCTCT and ChIP-R, CATGCACATGCAAAACACAG.

***In Utero* Electroporation.** Approximately 2 μl of DNA (4 μg/μL) were injected into the lateral ventricles and transferred into VZ cells by electroporation (five 50-ms pulses of 40 V at 950-ms intervals).

Further experimental details can be found in *SI Materials and Methods*.

ACKNOWLEDGMENTS. We thank M. Nobrega and L. Pennacchio for enhancer information, E. Jacobs and A. Campagnoni (UCLA), T. Iwasato (RIKEN Brain Science Institute), and M. Colbert (Cincinnati Children's Hospital Center) for providing mice, and R. Sears and R. DiLeone for help with hypothalamus anatomy. This study was supported by National Institutes of Health Grant NS054273, March of Dimes Foundation Grant 6-FY05-73, the Whitehall Foundation (N.S.), and the Canadian Institutes of Health Research (K.Y.K).

1. O'Leary D, Koester S (1993) Development of projection neuron types, axon pathways, and patterned connections of the mammalian cortex. *Neuron* 10:991–1006.
2. McConnell S (1995) Constructing the cerebral cortex: Neurogenesis and fate determination. *Neuron* 15:761–768.
3. Molyneaux B, Arlotta P, Menezes J, Macklis J (2007) Neuronal subtype specification in the cerebral cortex. *Nat Rev Neurosci* 8:427–437.
4. Angevine JJ, Sidman R (1961) Autoradiographic study of cell migration during histogenesis of cerebral cortex in the mouse. *Nature* 192:766–768.
5. Rakic P (1974) Neurons in rhesus monkey visual cortex: Systematic relation between time of origin and eventual disposition. *Science* 183:425–427.
6. Marin-Padilla M (1978) Dual origin of the mammalian neocortex and evolution of the cortical plate. *Anat Embryol (Berlin)* 152:109–126.
7. Rash B, Grove E (2006) Area and layer patterning in the developing cerebral cortex. *Curr Opin Neurobiol* 16:25–34.
8. Caviness VJ (1982) Neocortical histogenesis in normal and reeler mice: A developmental study based upon [3H]thymidine autoradiography. *Brain Res* 256:293–302.
9. Molyneaux B, Arlotta P, Hirata T, Hibi M, Macklis J (2005) Fezl is required for the birth and specification of corticospinal motor neurons. *Neuron* 47:817–831.
10. Arlotta P, *et al.* (2005) Neuronal subtype-specific genes that control corticospinal motor neuron development in vivo. *Neuron* 45:207–221.
11. Chen B, Schaevitz L, McConnell S (2005) Fezl regulates the differentiation and axon targeting of layer 5 subcortical projection neurons in cerebral cortex. *Proc Natl Acad Sci U S A* 102:17184–17189.
12. Chen J, Rasin M, Kwan K, Sestan N (2005) Zfp312 is required for subcortical axonal projections and dendritic morphology of deep-layer pyramidal neurons of the cerebral cortex. *Proc Natl Acad Sci USA* 102:17792–17797.
13. Smits P, *et al.* (2001) The transcription factors L-Sox5 and Sox6 are essential for cartilage formation. *Dev Cell* 1:277–290.
14. Lai T, *et al.* (2008) SOX5 Controls the sequential generation of distinct corticofugal neuron subtypes. *Neuron* 57:232–247.
15. Lefebvre V, Dumitriu B, Penzo-Méndez A, Han Y, Pallavi B (2007) Control of cell fate and differentiation by Sry-related high-mobility-group box (Sox) transcription factors. *Int J Biochem Cell Biol* 39:2195–2214.
16. Stolt C, *et al.* (2006) SoxD proteins influence multiple stages of oligodendrocyte development and modulate SoxE protein function. *Dev Cell* 11:697–709.
17. Gong S, *et al.* (2003) A gene expression atlas of the central nervous system based on bacterial artificial chromosomes. *Nature* 425:917–925.
18. Pennacchio L, *et al.* (2006) In vivo enhancer analysis of human conserved non-coding sequences. *Nature* 444:499–502.
19. Rice D, Curran T (2001) Role of the reelin signaling pathway in central nervous system development. *Annu Rev Neurosci* 24:1005–1039.
20. Heuer H, *et al.* (2003) Connective tissue growth factor: A novel marker of layer VII neurons in the rat cerebral cortex. *Neuroscience* 119:43–52.
21. McEvilly R, de Diaz M, Schonemann M, Hooshmand F, Rosenfeld M (2002) Transcriptional regulation of cortical neuron migration by POU domain factors. *Science* 295:1528–1532.
22. Hevner R, *et al.* (2001) Tbr1 regulates differentiation of the preplate and layer 6. *Neuron* 29:353–366.
23. Yoneshima H, *et al.* (2006) Er81 is expressed in a subpopulation of layer 5 neurons in rodent and primate neocortices. *Neuroscience* 137:401–412.
24. Nakagawa Y, O'Leary DD (2003) Dynamic patterned expression of orphan nuclear receptor genes *RORalpha* and *RORbeta* in developing mouse forebrain. *Dev Neurosci* 25:234–244.
25. Nieto M, *et al.* (2004) Expression of Cux-1 and Cux-2 in the subventricular zone and upper layers II-IV of the cerebral cortex. *J Comp Neurol* 479:168–180.
26. McConnell S, Ghosh A, Shatz C (1989) Subplate neurons pioneer the first axon pathway from the cerebral cortex. *Science* 245:978–982.
27. Kostovic I, Rakic P (1990) Developmental history of the transient subplate zone in the visual and somatosensory cortex of the macaque monkey and human brain. *J Comp Neurol* 297:441–470.
28. Jacobs E, *et al.* (2007) Visualization of corticofugal projections during early cortical development in a tau-GFP-transgenic mouse. *Eur J Neurosci* 25:17–30.
29. Bittencourt J, *et al.* (1992) The melanin-concentrating hormone system of the rat brain: An immuno- and hybridization histochemical characterization. *J Comp Neurol* 319:218–245.
30. Iwasato T, *et al.* (2008) Cortical adenylyl cyclase 1 is required for thalamocortical synapse maturation and aspects of layer IV barrel development. *J Neurosci* 28:5931–5943.
31. Rasin M, *et al.* (2007) Numb and Numbl are required for maintenance of cadherin-based adhesion and polarity of neural progenitors. *Nat Neurosci* 10:819–827.
32. Gerfen C (1989) The neostriatal mosaic: Striatal patch-matrix organization is related to cortical lamination. *Science* 246:385–388.
33. Alcamo E, *et al.* (2008) Satb2 regulates callosal projection neuron identity in the developing cerebral cortex. *Neuron* 57:364–377.
34. Britanova O, *et al.* (2008) Satb2 is a postmitotic determinant for upper-layer neuron specification in the neocortex. *Neuron* 57:378–392.
35. Jessell T (2000) Neuronal specification in the spinal cord: Inductive signals and transcriptional codes. *Nat Rev Genet* 1:20–29.

Supporting Information

Kwan *et al.* 10.1073/pnas.0806791105

SI Text

Plasmid Constructs. For *Sox5* expression, the full-length *Sox5* cDNA (BC110478) was inserted into pCAGEN. Luciferase reporter plasmids were made by inserting annealed 82-bp complementary oligonucleotides representing the wild-type (wt) and mutated (mut) SOX5 binding sites into the pGL3 promoter reporter plasmid (Promega) between BamHI and SalI restriction sites. The following oligonucleotide sequences were used for luciferase constructs:

wt top: gatcAATGAACTGTCAACAATCGGGCCA-TCCACAGAACCAGCATCACTCAAGAACTCGGCATTT-ACAGGCAACAAAGGATTGTCTG

wt bot: tcgaCAGACAATCCTTTGTTGCCTGTAAA-TGCCGAGTTCTTGAGTGATGCTGGTTCTGTGGAT-GGCCCGATTGTTGACAGTTCATT

mut1 top: gatcAATGAACTGTCAGCACTCGGGCCA-TCCACAGAACCAGCATCACTCAAGAACTCGGCAT-TTACAGGCAACAAAGGATTGTCTG

mut1 bot: tcgaCAGACAATCCTTTGTTGCCTGTAAA-TGCCGAGTTCTTGAGTGATGCTGGTTCTGTGGAT-GGCCCGAGTGCTGACAGTTCATT

mut2 top: gatcAATGAACTGTCAACAATCGGGCCA-TCCACAGAACCAGCATCACTCAAGAACTCGGCAT-TTACAGGCACCAGAGGATTGTCTG

mut2 bot: tcgaCAGACAATCCTCTGGTGCCTGTAAA-TGCCGAGTTCTTGAGTGATGCTGGTTCTGTGGAT-GGCCCGATTGTTGACAGTTCATT

mut3 top: gatcAATGAACTGTCAGCACTCGGGCCA-TCCACAGAACCAGCATCACTCAAGAACTCGGCATT-TACAGGCACCAGAGGATTGTCTG

mut3 bot: tcgaCAGACAATCCTCTGGTGCCTGTAAA-TGCCGAGTTCTTGAGTGATGCTGGTTCTGTGGATG-GCCCGAGTGCTGACAGTTCATT

mut4 top: gatcGACGAGCTGTCAGCACTCGGGCCA-TCCACAGAACCAGCATCACTCAA-GAACTCGGCATTTACAGGCACCAGAGGCTCACATG

mut4 bot: tcgaCATGTGAGCCTCTGGTGCCTGTA-AATGCCGAGTTCTTGAGTGATGCTGGTTCTGTGG-ATGGCCCGAGTGCTGACAGCTCGTC

Axonal Tracing. For *in vivo* retrograde tracing, fluorescent microbeads (Lumafluor) were injected into targeted regions in P3 mice. After recovery and survival for 4 days, brains were perfused and immunostained for SOX5. For axonal tracing in fixed brains, P0 brains were cut sagittally along the midline, and DiI crystals were inserted into the thalamus. Brains were incubated at 37°C in sterile PBS for 8–10 weeks before analysis.

Quantitative RT-PCR. Total RNA was isolated from freshly microdissected cortices using RNeasy minikit (Qiagen), and cDNA was synthesized using SuperScript (Invitrogen). For quantitative RT-PCR, predesigned primer and probe sets were obtained from Applied Biosystems. Thermocycling was carried out using the Applied Biosystems 7900 system. *Gapdh* levels were used for normalization.

Histology. Mice P7 or older were perfused with 4% paraformaldehyde (PFA), dissected, and fixed by immersion in PFA overnight at 4°C. Embryonic and neonatal brains were dissected and fixed by immersion in PFA overnight at 4°C. Mouse brains were sectioned at 70 μm with a Vibratome VT1000S (Leica) for immunostaining or were cryoprotected in graded sucrose solutions, frozen, and cryosectioned at 40 μm or 60 μm for *in situ* hybridization. Human fetal brains at 21 and 22 weeks of gestation were obtained from the Human Fetal Tissue Repository of the Albert Einstein College of Medicine under the guidelines approved by the Yale Institutional Review Board, fixed by immersion in 4% PFA for 36 h, cryoprotected, frozen, and cryosectioned at 60 μm. For immunostaining, brain sections were incubated in blocking solution containing 5% normal donkey serum (Jackson Immuno Research Laboratories), 1% BSA, 0.1% glycine, 0.1% lysine, and 0.3% TritonX-100 in PBS for 1 h. Sections then were incubated for 16 h at 4°C in primary antibodies diluted in blocking solution, washed, and incubated with the appropriate fluorescent secondary antibodies or processed for immunohistochemistry. The following primary antibodies and dilutions were used: anti-CldU (Accurate Chemical/Rat/1:100); anti-IdU (BD Biosciences/Mouse/1:200); anti-BCL11B (Abcam/Rat/1:500); anti-CUTL1 (Santa Cruz Biotechnology/Rabbit/1:100); anti-ETV1 (Abcam/Rabbit/1:3000); anti-GFP (Molecular Probes/Rabbit/1:2000); anti-β-galactosidase (LacZ) (MP Biomedicals/Rabbit/1:20000); anti-MAP2 (EnCor Biotech/Chicken/1:250); anti-MCH (gift of Ralph DiLeone and Robert Sears/Rabbit/1:5000); anti-RELN (Chemicon/Mouse/1:1000); anti-SOX5 (Genway/Rabbit/1:100 or Santa Cruz Biotechnology/Goat/1:200); anti-TBR1 (Chemicon/Rabbit/1:1000); and anti-ZFPM2 (Santa Cruz Biotechnology/Rabbit/1:250).

For *in situ* hybridization, cryosections or whole mounts were hybridized using digoxigenin (DIG)-labeled riboprobes for mouse *Ctgf*, mouse *Tle4*, mouse *Fezf2*, and human *FEZF2.* Hybridization was performed overnight at 60°C or 70°C, and the signal was detected with an alkaline phosphatase-conjugated anti-DIG antibody and nitro blue tetrazolium chloride/bromo-4-chloro-3-indolyl phosphate (NBT/BCIP) (Roche Applied Science).

CldU and IdU Labeling. Timed-pregnant mice were injected i.p. with CldU or IdU (Sigma) at 0.05 mg per g of body weight. Mice were analyzed for incorporation of CldU and IdU using appropriate antibodies.

Quantitative Analysis. Data were analyzed by two-tailed Student's *t*-tests with a significance level of at least $P < 0.05$ for all statistical comparisons. Numbers of replicates are given in the main text or figure legends. To quantify the distribution of neurons, the P0 cortex was divided radially into 10 equal bins from the pia to the upper edge of the white matter. For E14.5 analyses, the pia to the upper edge of the intermediate zone was divided radially into five bins. Cells in each bin were quantified and reported as percentage of total cells counted.

1. Pennacchio L, *et al.* (2006) In vivo enhancer analysis of human conserved non-coding sequences. *Nature* 444:499–502.
2. Iwasato T, *et al.* (2000) Cortex-restricted disruption of NMDAR1 impairs neuronal patterns in the barrel cortex. *Nature* 406:726–731.
3. Kawamoto S, *et al.* (2000) A novel reporter mouse strain that expresses enhanced green fluorescent protein upon Cre-mediated recombination. *FEBS Lett* 470:263–268.
4. Iwasato T, *et al.* (2008) Cortical adenylyl cyclase 1 is required for thalamocortical synapse maturation and aspects of layer IV barrel development. *J Neurosci* 28:5931–5943.

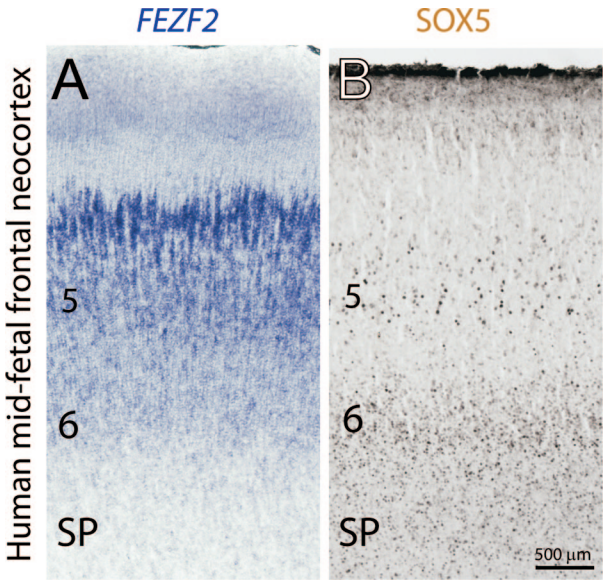

Fig. S1. *FEZF2* and SOX5 expression in subplate and deep layers of the human mid-fetal frontal neocortex. Expression of *FEZF2* and SOX5 in 22 weeks of gestation human neocortex was detected with DIG-labeled riboprobes (*A*) and immunostaining (*B*), respectively. *FEZF2* is highly expressed in L5 and to a lesser extent in L6 and SP. SOX5 is expressed highly in SP and L6 and in the deep parts of L5.

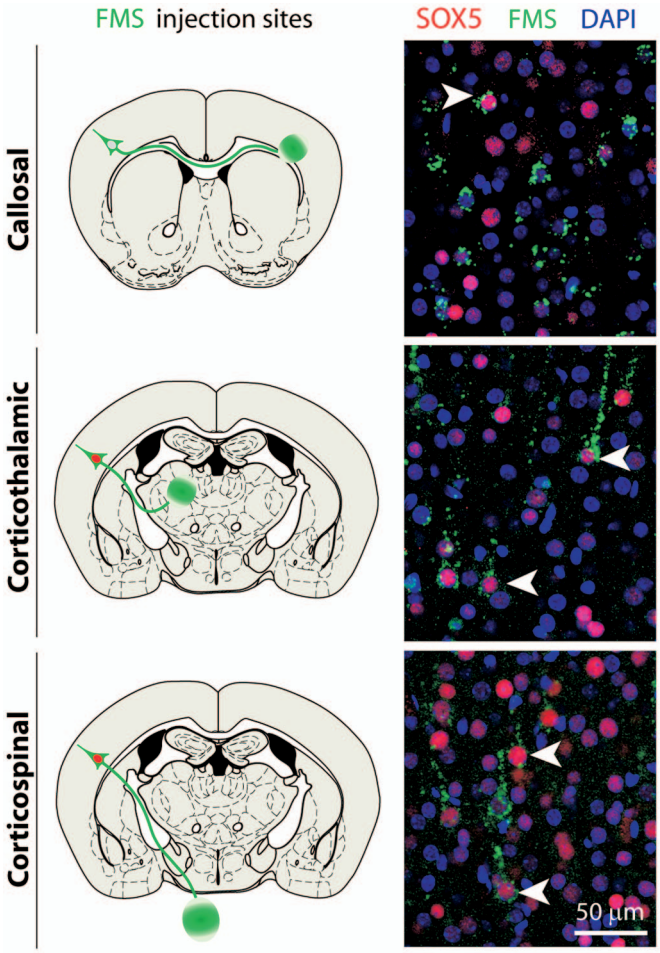

Fig. S2. SOX5 is expressed by cortical projection neurons of multiple projection subclasses. *In vivo* retrograde axonal tracing using fluorescent latex microspheres (FMS) (*green*). After FMS injections into the contralateral neocortex/white matter, ipsilateral thalamus, and cervical spinal cord at P3, cortical sections were stained immunofluorescently for SOX5 at P7. (*Left*) Schematic depictions of stereotaxic injection sites of FMS and normal projection routes (*green*). (*Right*) Representative images of neurons (*arrowheads*) in the P7 cortex retrogradely labeled with FMS (*green*) and co-labeled by SOX5 (*red*). SOX5 was expressed by a great majority of corticothalamic and corticospinal neurons in the deep layers (91.0% ± 2.6% and 81.5% ± 1.4%, respectively). SOX5 was also localized to a small number of FMS-positive callosal projection neurons in the deep layers (11.6% ± 1.4%).

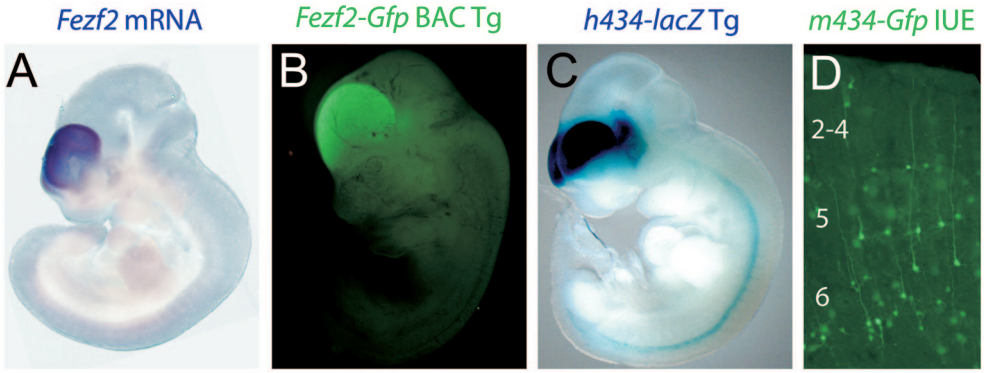

Fig. S3. The activity of the human 434 enhancer and its mouse orthologue closely mimicked the expression of *Fezf2*. (*A*) E10.5 whole mount hybridized with a riboprobe for *Fezf2*. (*B*) E12.5 whole mount of unstained *Fezf2-Gfp* transgenic mouse. (*C*) LacZ histochemistry of E11.5 whole mount of transgenic mouse expressing lacZ under the control of the 434 enhancer (four out of four founders) (Image courtesy of Marcelo Nobrega and Len Pennacchio; additional data available at http://enhancer.lbl.gov.) (1). (*D*) Cortical section of P7 brain electroporated *in utero* at E12.5 with a construct expressing GFP under the control of the mouse 434 enhancer. During early embryonic ages, the activities of the *Fezf2-Gfp* transgene and the human 434 enhancer closely mimic the endogenous expression of *Fezf2*. At P7, the mouse orthologue of the 434 enhancer showed activity in the deep cortical layers, similar to endogenous *Fezf2*.

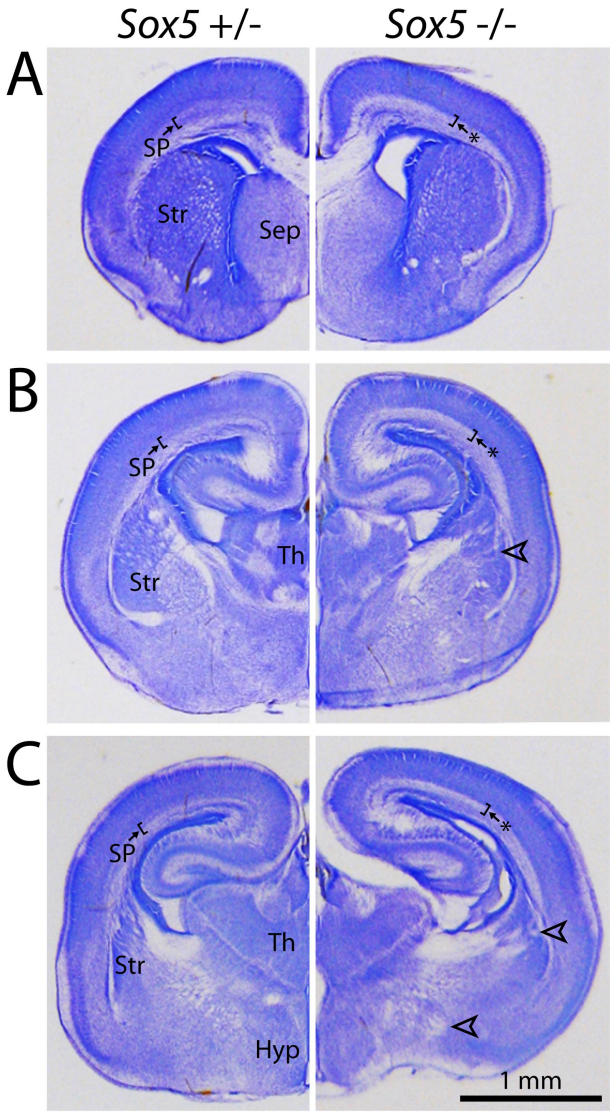

Fig. S4. Cytoarchitectural organization of the P0 *Sox5* Het (+/−) and KO (−/−) forebrain. Nissl staining of P0 coronal sections of *Sox5*+/− and *Sox5*−/− brains at the levels of the septum/callosum/striatum (*A*), hippocampus/internal capsule (*B*), and thalamus (*C*) revealed abnormalities in cytoarchitecture of the *Sox5*−/− forebrain. The thickness of the *Sox5*−/− neocortex is slightly reduced because of the absence a clearly delineated SP immediately above the white matter. Asterisks denote the expected location of the SP in *Sox5*−/− neocortex. Nissl staining also revealed defects in axon projections, including aberrant axon tracts and defasciculated bundles (*arrowheads*) in septum (Sep), striatum (Str), and hypothalamus (Hyp) of *Sox5*−/− mice. Th, thalamus.

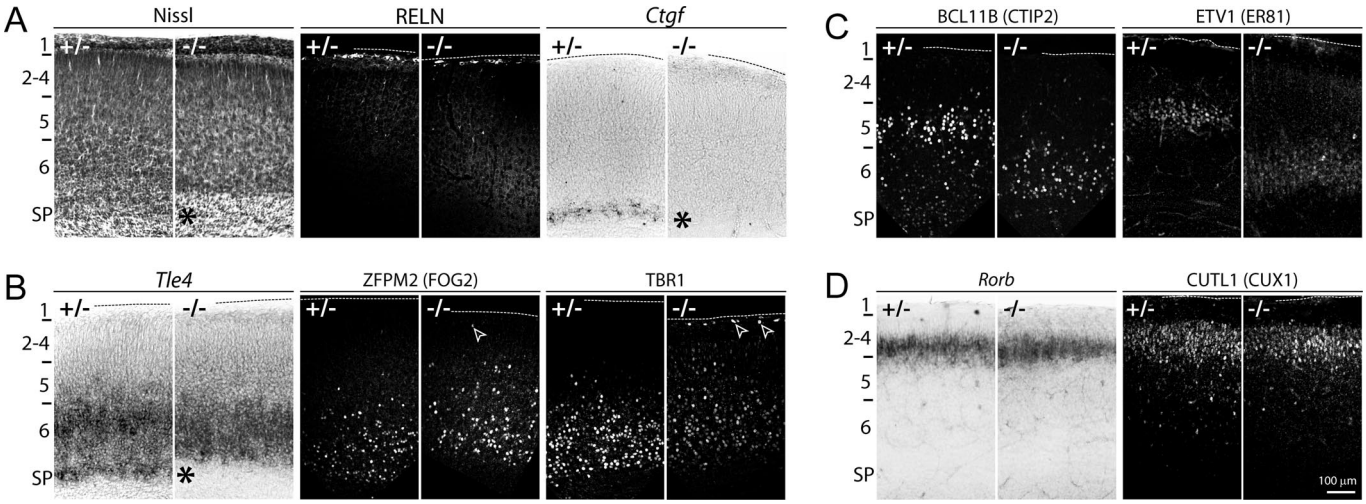

Fig. S5. Alterations in laminar-specific marker expression in *Sox5* KO neocortex. Neocortical tissue sections were Nissl-stained or immunostained as indicated or hybridized using the indicated riboprobe. Dashed lines indicate the pial surface. The expected location of SP in KO neocortex is indicated (asterisks). (*A*) Nissl staining reveals absence of a well-delineated SP in the *Sox5*−/− mice. RELN, a marker of Cajal-Retzius neurons in L1, is largely unaffected. The expression of *Ctgf*, a marker of SP neurons, is severely reduced. (*B*) *Tle4* is expressed in deep neocortex but is absent from the expected location of SP in *Sox5*−/− mice. The expression levels of two SP and L6 markers, ZFPM2 and TBR1, are markedly reduced in *Sox5*−/− mice. Ectopic ZFPM2-positive and TBR1-positive cells (*arrowheads*) are present at the upper edge of L2. (*C*) Expression of L5 markers BCL11B and ETV1 is shifted to deeper laminar positions, immediately bordering the white matter, in *Sox5*−/− mice. (*D*) The expression of upper layer markers *Rorb* (L4) and CUTL1 (L2–4) is unaffected in *Sox5*−/− mice.

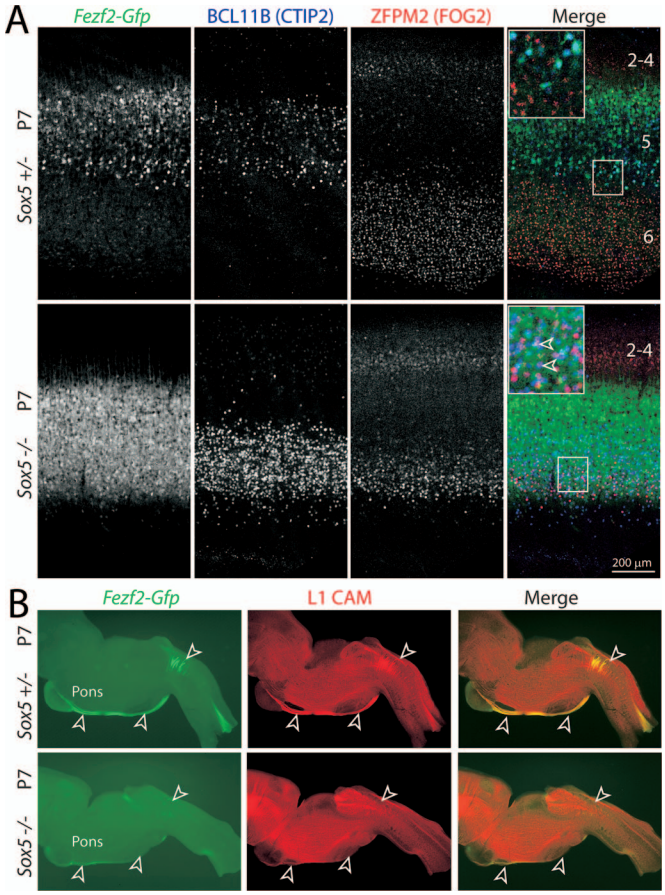

Fig. S6. Abnormal mixed molecular properties of deep-layer neurons and loss of subcerebral/corticospinal projections persisted in P7 *Sox5* KO mice. (*A*) Sections of P7 brains double-immunostained as indicated. In the deep layers of the *Sox5*+/− neocortex, ZFPM2 (*red*) showed minimal co-expression with BCL11B (*blue*) and *Fezf2-Gfp* (*green*). In contrast, in the deeper part of the *Sox5*−/− neocortex, ZFPM2, BCL11B, and *Fezf2-Gfp* were coexpressed extensively (*arrowheads*), indicating that changes in neuronal molecular identity in the *Sox5*−/− neocortex persist at later postnatal stages. (*B*) The corticospinal tracts in P7 *Sox5*+/− and *Sox*−/− brains were examined. Sagittal sections were immunostained for L1-CAM (*red*), a marker of axon tracts. L1-CAM-positive and *Fezf2-Gfp*-positive (*green*) corticospinal axons (*arrowheads*) were severely diminished in the P7 *Sox5*−/− brains.

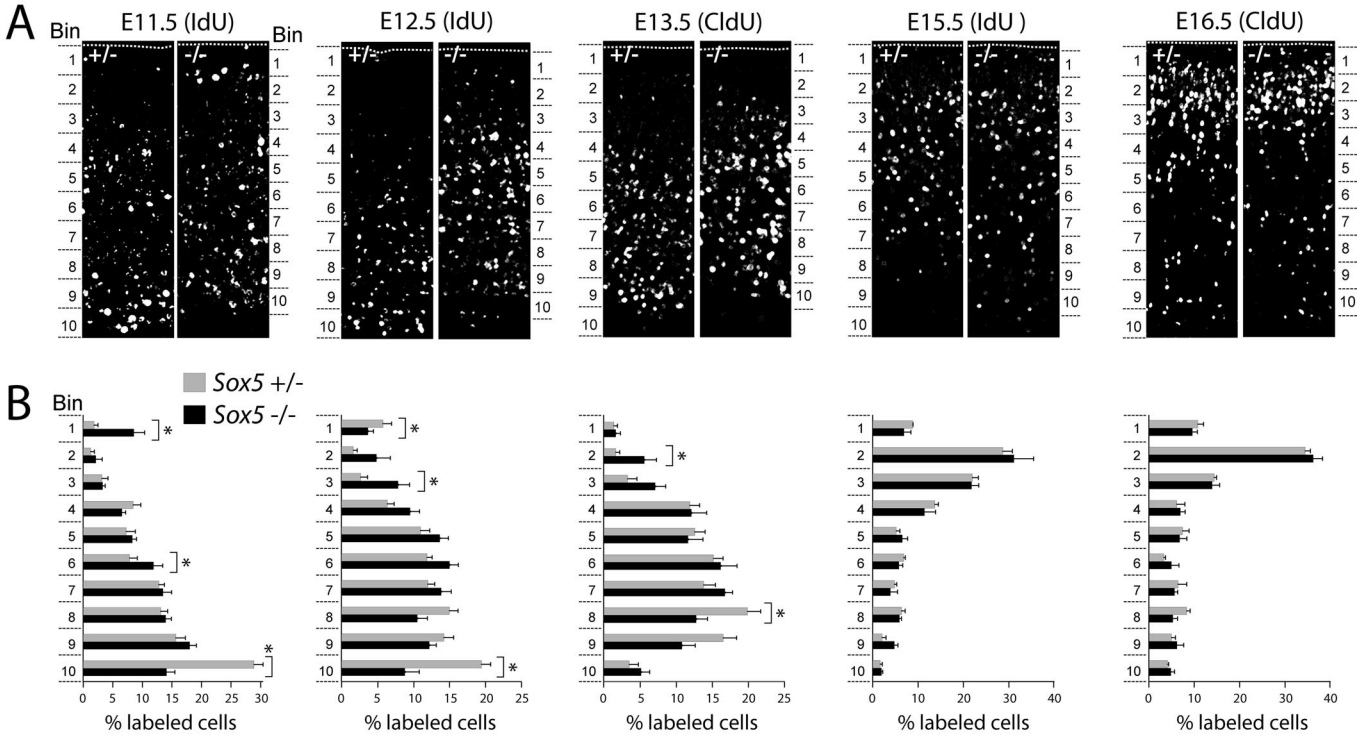

Fig. S7. Thymidine analogue birthdating reveals specific migration defects restricted to SP and deep-layer neurons of *Sox5* KO neocortex. (*A*) P0 sections of *Sox5*+/− and *Sox5*−/− neocortices of mice injected with a thymidine analogue (IdU or CldU) at the indicated age were immunostained using antibodies specific for IdU or CldU. Dashed lines indicate the pial surface. (*B*) Quantification of radial distributions of labeled cells. In *Sox5*−/− neocortex, the distribution of early-born cells (E11.5–E13.5) was shifted toward more superficial positions. There was a severe reduction in cells labeled at E11.5 and E12.5 occupying the deepest bin (Bin 10). The number of E11.5-labeled cells in L1 (Bin 1) was increased significantly, consistent with defects in PP splitting. Although the distribution of cells labeled at E13.5 showed a small shift toward more superficial layers, the distribution of cells labeled at E15.6 and E16.5 was unaffected in the *Sox5*−/− neocortex. Error bars represent S.E.M. Student's *t* test, $*P < 0.05$.

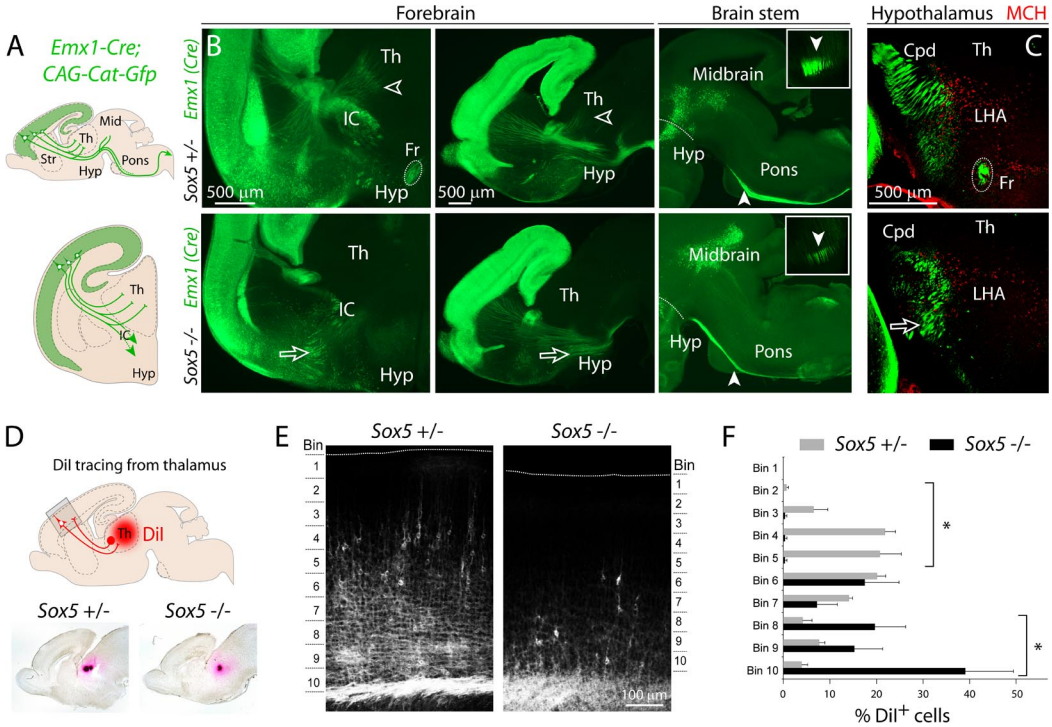

Fig. S8. Pan-cortical anterograde tracing and DiI retrograde tracing from dorsal thalamus in *Sox5* KO mice. (*A*) Schematic depictions showing subcortical *Emx1-Cre;CAG-Cat-Gfp*-positive axons (*green*) (2–4) arising from cortical projection neurons of all layers and subtypes. (*B*, *C*) P0 coronal and sagittal sections of *Sox5*+/− and *Sox5*−/− brains doubly heterozygous for *Emx1-Cre;CAG-Cat-Gfp*. (*B*) The *Sox5*+/− brain exhibited a loss of stereotypical internal capsule (IC) organization, a dramatic decrease in the number of GFP-positive axons in the corticothalamic tract (*open arrowheads*) and fornix (Fr), and an aberrant axon tract in the hypothalamus (Hyp) (*arrows*). In *Sox5*−/− mice, GFP-positive subcerebral axons were severely reduced and confined to a few thin bundles (*solid arrowheads*), as confirmed by coronal sections of the pons (*Inset; solid arrowheads*). (*C*) Coronal sections through the caudal cerebrum immunostained for melanin-concentrating hormone (MCH) (*red*), a marker of the lateral hypothalamic area (LHA). In *Sox5*−/− mice, the GFP-positive axons deviated from the IC and cerebral peduncle (Cpd) and aberrantly entered the LHA (*arrow*). (*D*) Schematic depiction of DiI retrograde tracing from the thalamus and representative location of DiI placement. (*E*) Sagittal sections of DiI-labeled P0 brains of the indicated genotype. DiI-labeled corticothalamic and thalamocortical axons are present underneath the neocortex. Retrogradely labeled corticothalamic neurons in the *Sox5*+/− cortex were distributed in L5 and L6. In the *Sox5*−/− neocortex there was a marked decrease in the number of retrogradely labeled neurons, and their distribution was shifted toward deeper laminar positions. (*F*) Quantification of the radial distribution of DiI-labeled neurons. Error bars represent S.E.M. Student's *t* test, $*P < 0.05$.

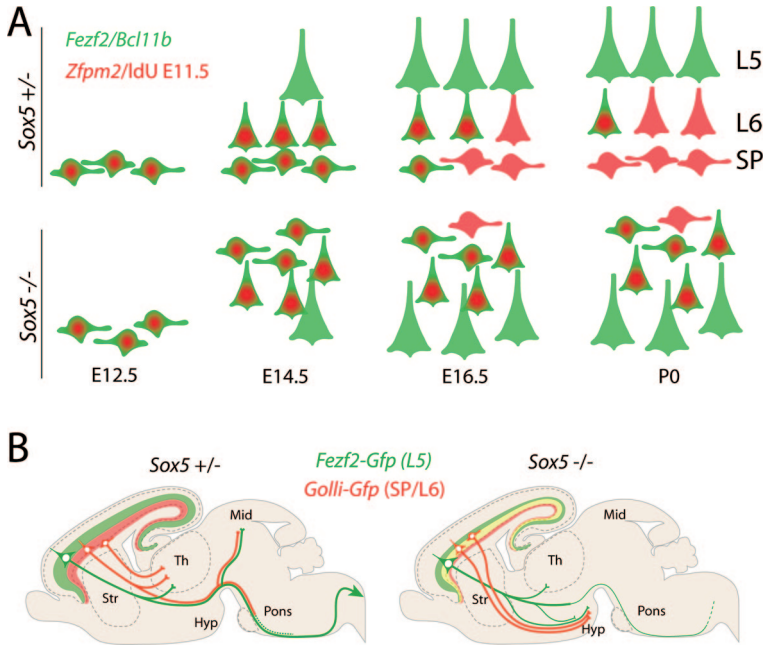

Fig. S9. Summary of defects in molecular differentiation and axonal projections in *Sox5* KO mice. (*A*) Schematic of progressive postmigratory refinement of L5 (*green*) and L6 and SP (*red*) molecular properties. At E12.5 and E14.5, newly postmigratory SP and L6 neurons expressed high levels of *Fezf2* and BCL11B. By E16.5, these markers were expressed by a small proportion of SP and L6 neurons. By P0, the L5-enriched patterns of these markers are assumed. In the *Sox5*−/− neocortex, this downregulation failed, resulting in abnormal maintenance of *Fezf2* and BCL11B in SP and L6 neurons. (*B*) Schematic of *Fezf2-Gfp*-positive and *Golli-Gfp*-positive subcortical axons in *Sox5*+/− and *Sox5*−/− mice. *Fezf2-Gf-positive* axons, arising mostly from L5 neurons, are severely reduced in dorsal thalamus and subcerebral structures and are partially misrouted to the hypothalamus in *Sox5*−/− mice. *Golli-Gfp*-positive axons, originating mostly from L6 and SP neurons, are nearly completely absent from dorsal thalamus and subcerebral structures and are entirely misrouted to the hypothalamus.